

Lawrence Berkeley National Laboratory

LBL Publications

Title

Mechanical vs Electronic Strain: Oval-Shaped Alkynyl-Pt(II)-Phosphine Macrocycles

Permalink

<https://escholarship.org/uc/item/1f19t1qf>

Journal

Organometallics, 38(24)

ISSN

0276-7333

Authors

Plutnar, Jan

Givelet, Cecile

Lemouchi, Cyprien

et al.

Publication Date

2019-12-23

DOI

10.1021/acs.organomet.9b00633

Peer reviewed

Mechanical vs. Electronic Strain: Oval-Shaped Alkynyl-Pt(II)-Phosphine Macrocycles

Jan Plutnar,^a Cecile Givelet,^{a,b} Cyprien Lemouchi,^{a,b} Jana Dyrtrtová-Jaklová,^a Ivana Císařová^c, Simon J. Teat^d and Josef Michl^{a,b*}

[a] *Institute of Organic Chemistry and Biochemistry, Academy of Sciences of the Czech Republic, Flemingovo nám. 2, 16610 Prague 6, Czech Republic*

[b] *Department of Chemistry, University of Colorado, Boulder, CO 80309-0215, United States*

[c] *Department of Inorganic Chemistry, Faculty of Science, Charles University in Prague, Hlavova 2030, 12843 Prague 2, Czech Republic*

[d] *Advanced Light Source, Berkeley Laboratory, 1 Cyclotron Road, Berkeley, California, 94720, United States*

Abstract. Pyridine-terminated molecular rods and either (i) the *cis*-(dppp)(I)Pt(C≡C-triptycene-C≡C)Pt(I)(dppp) rod or (ii) the *trans*-(PEt₃)₂(I)Pt(C≡C-biphenyl-C≡C)Pt(I)(PEt₃)₂ rod assemble into macrocycles, characterized by NMR, IMS-ESI, and in two cases also single crystal X-ray diffraction. The former form rectangles with bidentate phosphine-containing *cis*-coordinated Pt(II)-alkyne corners. In the latter, the preference of the Pt centers for *trans* configuration overrules the preference of the triple bonds for linearity and NMR shows that they have oval structures with alternating bent rod and bent *trans* (C≡C)(Py)Pt(PEt₃)₂ components, in agreement with density functional theory calculations.

Introduction

Organometallic platinum(II)-acetylide complexes have attracted the attention of researchers for over forty years. The development of this area was accelerated by Sonogashira's discovery of a simple synthesis of di(phosphine)di(alkynyl)Pt(II) and di(phosphine)(alkynyl)(halo)Pt(II) complexes using a Cu(I) halide and secondary amine-based catalyst.^{1,2} Although the formation of both *cis* and *trans* isomers is possible, depending on temperature and solvent,¹ in most cases the *trans* isomer of the Pt(II) complex is formed exclusively. The availability of these *trans* isomers makes them the preferred building blocks in the construction of platinum(II)-based supramolecular structures. The almost linear arrangement of the C-Pt-C environment requires the introduction of a shape-forming structural unit to assemble a cyclic compound. Most often, a clip-type acceptor is combined with a linear donor, and the shape of the resulting macrocycle is determined by the shape of the bridging ligand with acetylide functionalities. This combination usually yields rectangular^{3,4} and sometimes triangular⁵ complexes. The bridging donors often are pyridines^{3,4,5,6,7,8,9} or carboxylates,^{10,11,12,13} but other ligands have also been used.¹⁴ The reverse approach, a self-assembly of a linear acceptor with a clip-type donor, is possible, too.^{15,16}

Although the synthesis of the *cis* isomers of di(phosphine)di(alkynyl)Pt(II) complexes is more demanding than that of the *trans* isomers, they, too, have been used for the formation of macrocycles. The procedure requires a stepwise construction and careful control of reaction conditions^{17,18} in order to prevent formation of multinuclear zig-zag oligomers.¹⁹ In addition to Sonogashira's original procedure for the preparation of the *cis* complexes, an alternative consisting of a ligand-exchange reaction of a preformed *trans*-bis(triphenylphosphine) complex with a bidentate phosphine was developed and several examples of its application were reported.^{20,21}

In order to make the use of the *cis* isomers in the self-assembling reactions possible, the *cis*-di(phosphine)(alkynyl)(halo)Pt(II) complex has to be prepared first. While this is difficult to achieve for monodentate phosphines, complexes containing 1,2-bis(dimethylphosphino)ethane (dmpe) and 1,3-bis(diphenylphosphino)propane (dppp) were synthesized by oxidative addition

of an alkynyliodonium salt to $\text{Me}_2\text{Pt}(\text{dmpe})$ followed by reductive elimination of ethane²² or by Sonogashira's original procedure.¹ Trigonal cage-shaped trimetallic macrocycles were formed with 1,3,5-tris(4-pyridylethynyl)benzene.^{23,24} The use of three-dimensional macrocycles for the construction of longitudinal surface-mounted molecular rotors²⁵ is our long-term interest and it generally requires the participation of a more than bidentate donor.

In an effort to improve the control of the synthesis of sturdy structures via self-assembly, we briefly communicated an extension of the reverse formation of covalent macrocycles to a two-step process.¹⁶ First, pyridine-terminated rods were reversibly self-assembled with binuclear Pt-terminated rods to charged supramolecular macrocycles via dative $\text{N}\rightarrow\text{Pt}^+$ bonds. Second, covalent stabilization under preservation of topology was achieved by replacement of the pyridine-terminated rods with 4,4'-diethynylbiphenyl rods, in which the labile dative $\text{N}\rightarrow\text{Pt}^+$ bonds are converted to sturdy uncharged covalent C-Pt bonds. The two-step procedure combines the facility and high yield of self-correcting reversible assembly with the robustness of covalent synthesis. At the time, we took it for granted that the resulting covalent macrocycles had to contain *cis* $(\text{C}\equiv\text{C})_2\text{Pt}(\text{PEt}_3)_2$ centers and had rectangular shape with the P atoms in the plane of the ring, since the *trans* arrangement of the alkynes at the Pt atoms would be too strained. Prompted by results of density functional theory (DFT) calculations, we realized more recently that in this case the preference of the Pt centers for *trans* configuration overrules the resistance of triple bonds to bending, and that the macrocycles actually have a rather unusual oval structure containing *trans* $(\text{C}\equiv\text{C})_2\text{Pt}(\text{PEt}_3)_2$ centers, with the P atoms above and below the ring.

Results

(i) Cis Dialkynyl-Pt(II)-Diphosphine Macrocycles and Their Datively Bonded Precursors. The diphosphine ligand forces a *cis* arrangement at the Pt atom and dictates the nature of the self-assembled structures.

Rods. We prepared two Pt-terminated rods for the self-assembly and characterized both by single-crystal X-ray diffraction. The first rod is the already known²⁴ triptycene-9,10-diethynylbis{*cis*-[bis(diphenylphosphino)propane]iodoplatinum(II)} (**1**, Chart 1), obtained in a mediocre yield by treatment of a fourfold stoichiometric excess of 9,10-diethynyltriptycene (**2**) with *cis*-[bis(diphenylphosphino)propane]platinum(II) diiodide (*cis*-dppp)PtI₂ (**3**) under Sonogashira¹ coupling conditions. Before self-assembly, the Pt centers were activated by replacement of the iodide with the nitrate anion or with pyridine.

A similar reaction of 2,5-bis(trimethylsilyl)-1,4-diethynylbenzene (**4**) with **3** produced a low yield of the other rod, 2,5-bis(trimethylsilyl)phenyl-1,4-diethynylbis{*cis*-[bis(diphenylphosphino)propane]platinum(II)} (**5**).

The rod **1** crystallizes in monoclinic space groups $\text{P2}_1/c$ (**1a**, from $\text{CH}_2\text{Cl}_2/\text{THF}$) and $\text{P2}_1/n$ (**1b**, from CH_2Cl_2). One rod molecule per structural unit is present in **1a** and two are present in **1b**, together with five highly disordered molecules of methylene chloride (Figures S71-S73 in Supporting Information). The Pt atom is in a nearly perfect square-planar environment. The main difference in rod structure between **1a** and **1b** is the I-Pt-Pt-I torsion angle, -78.28 and 133.81° in the former, and 109.15° in the latter.

The rod **5** crystallizes in triclinic space group P1 with one rod molecule and two distorted DMF molecules per structural unit (Figure S74 in Supporting Information). As in **1**, the Pt atom is in a nearly ideal square-planar environment. The center of the rod resides at an inversion center and the I-Pt-Pt-I torsional angle is 180° . The van der Waals radii packing image reveals close contacts between the TMS groups and the phenyl groups of the dppp ligands.

Datively Bonded Rectangles. A replacement of the iodide anion in the rod **1** with nitrate followed by reaction with di(4'-pyridyl)acetylene (**6**) or di(4'-pyridyl)butadiyne (**7**) resulted in the formation of non-covalent rectangles **8** and **9** (Scheme 1). Analogous reactions of the rod **5** with **6** or **7** always yielded a linear polymer and no rectangles were isolated or detected

(Scheme 2).

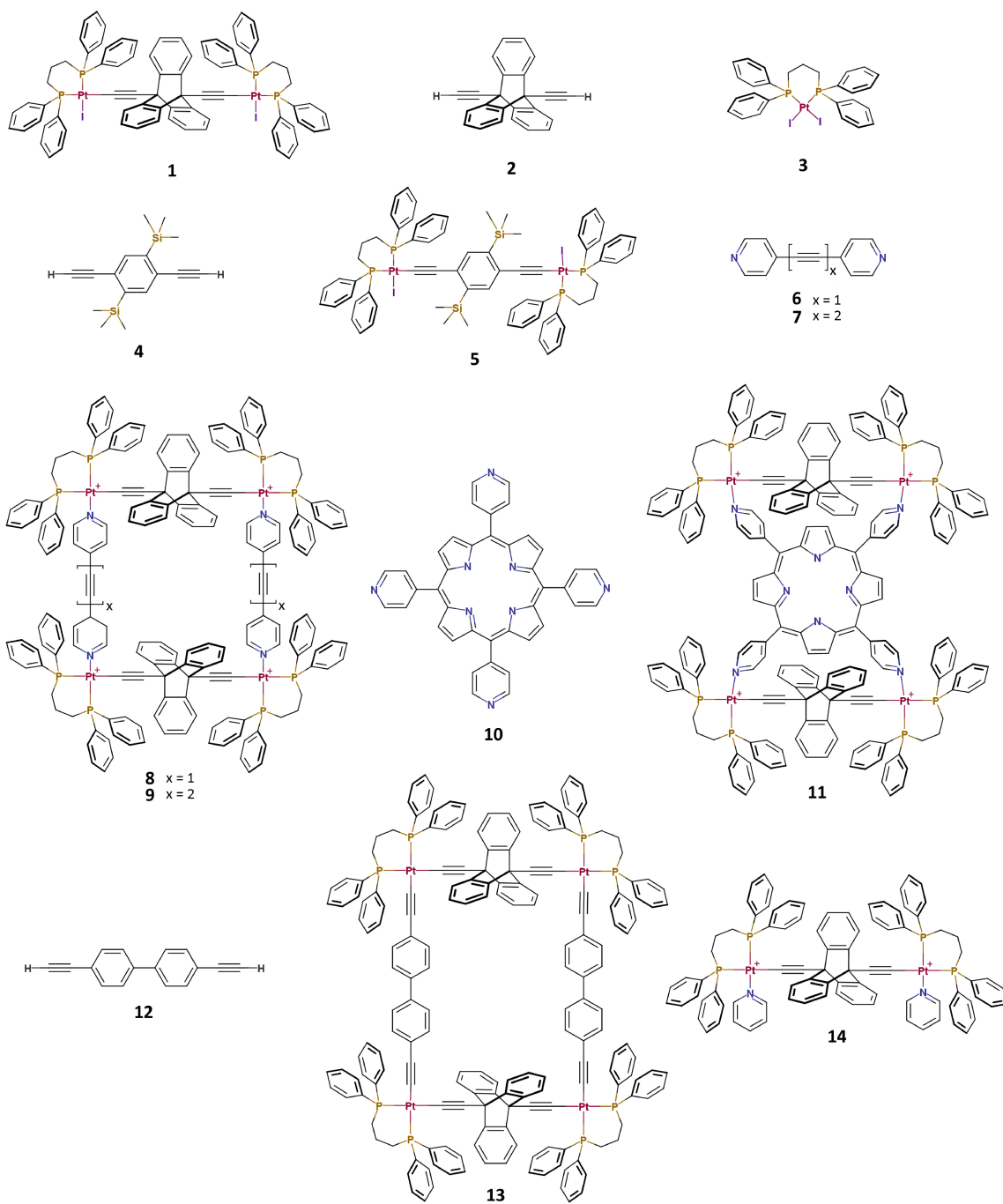
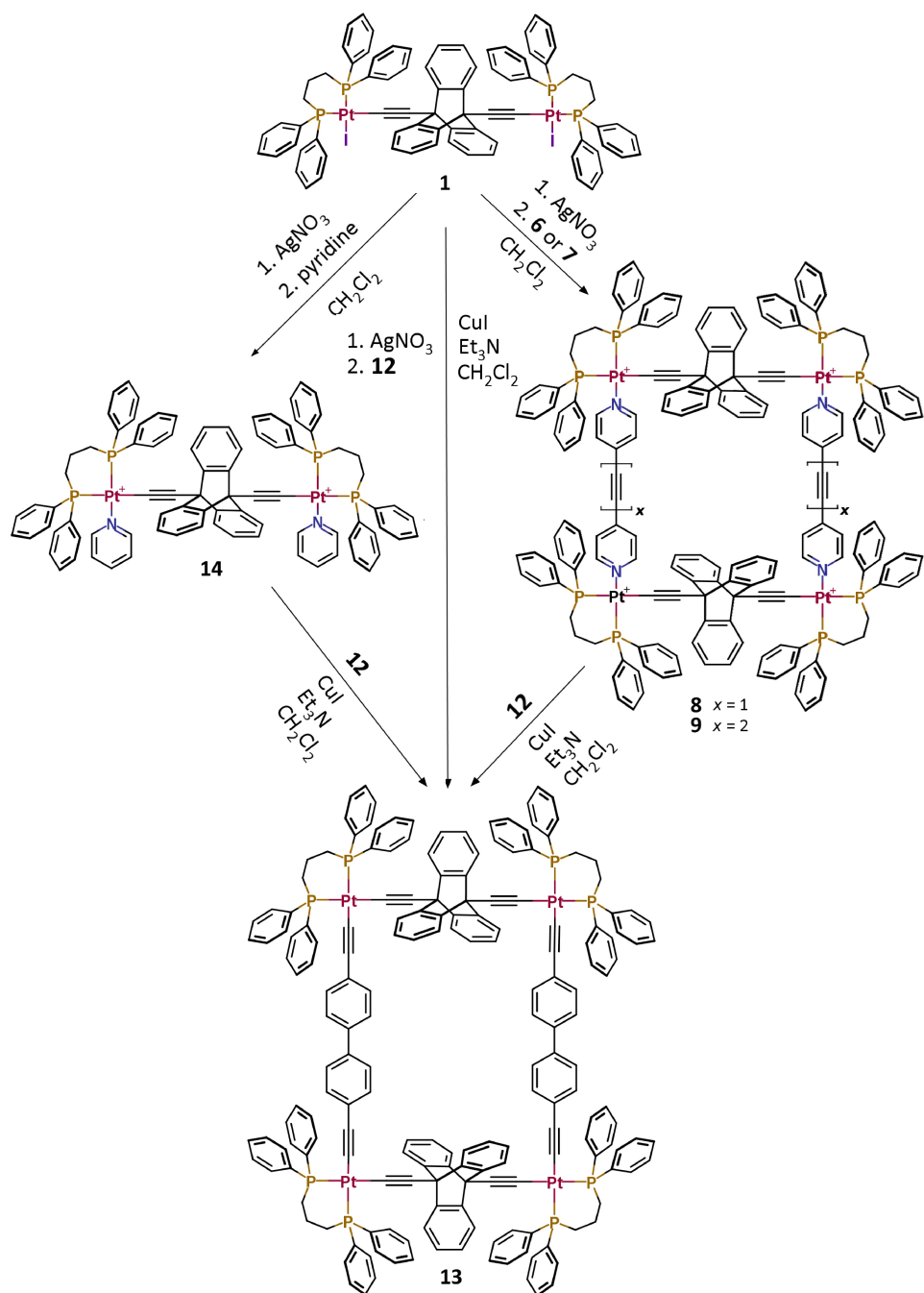
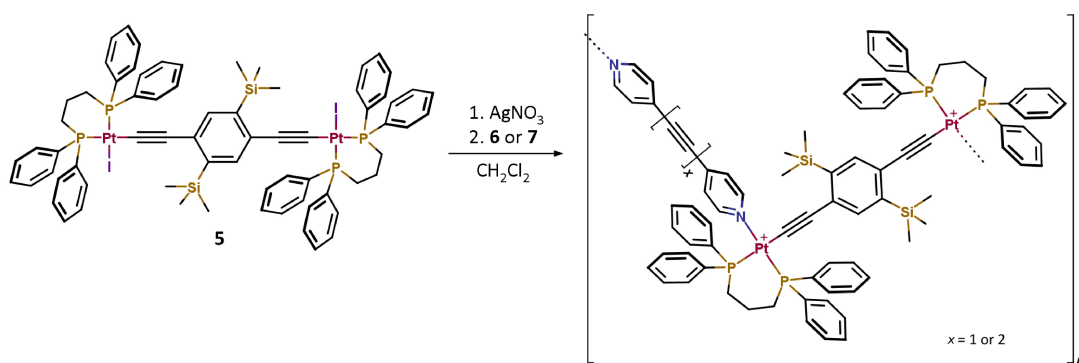


Chart 1. Structures of reagents and products.



Scheme 1. Reaction pathways from **1** to **13** (nitrate anions are not shown).



Scheme 2. Formation of oligomers from **5** (nitrate anions are not shown).

The structure of the rectangular complexes **8** and **9** was deduced from an examination of their NMR and mass spectra. The rectangle **9** exhibits a set of two P-P doublets ($^2J_{\text{P-P}} = 28$ Hz) in the solution ^{31}P NMR spectrum, accompanied by two sets of ^{195}Pt satellites. The Pt-P coupling constants were used as a diagnostic tool for evaluation of the coordination environment of the platinum(II) center.²⁶ The signal at -10.64 ppm has two satellites with $^1J_{\text{Pt-P}} = 3142$ Hz indicating the presence of a P atom trans to the pyridyl ligand. The $^1J_{\text{Pt-P}} = 2210$ Hz value of the signal located at -0.54 ppm corresponds to a P atom trans to the alkyne (Figure 1). The ^1H and ^{13}C NMR signals of the dppp ligand are split into two sets due to the decreased symmetry in the complex. A combination of ^1H - ^{31}P and ^1H - ^{13}C correlation experiments allowed us to assign all the signals in the proton and carbon spectra to the structure (Figures S29 – S32 in the Supporting Information). The assigned cyclic structure follows from the absence of any ^1H NMR signal that could be assigned to a non-coordinated terminus of **7** and the absence of any ^{31}P NMR signal attributable to an environment found in the starting nitrate version of **1**.²⁴

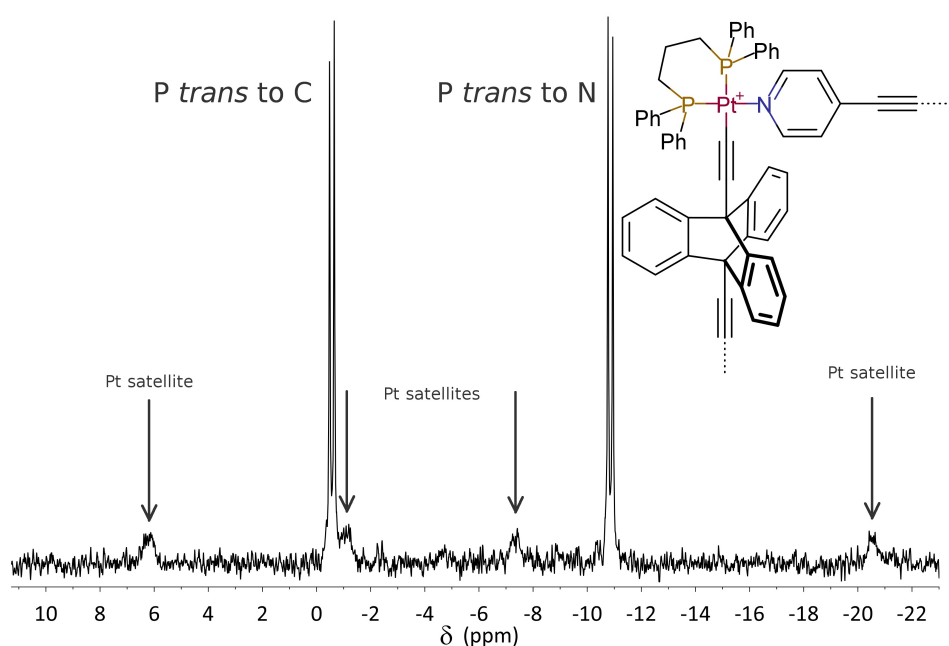


Figure 1. The ^{31}P NMR spectrum of **9**. ^{195}Pt satellites are marked with arrows.

However, any larger macrocycle formed from the same components would exhibit the same NMR spectra. To determine the actual size of the molecule, we used electrospray ionization/ion mobility spectrometry (ESI-IMS). The mass spectrum contains six major peak envelopes. The most intense signal at $m/z = 1166.8$ corresponds to an ion pair of the tetracation **9** and NO_3^- . The free tetracation **9** is located at 859.5, together with a dication of a fragment that corresponds to one-half of the molecule. An additional peak corresponding to the nitrate dication ion pair was found at 1781.2. No fragments with charge higher than 4+ were observed. In all cases the isotopic pattern envelopes corresponded to the shapes expected for the postulated elemental composition and the peak separation fitted the calculated charge of the fragment (Figures S64-S67 in the Supplementary Information).

The smaller rectangle **8** exhibits spectroscopic patterns very similar to those of **9**. Two P-P doublets are present in the ^{31}P NMR spectrum at -10.65 ($^1J_{\text{Pt-P}} = 3152$ Hz, $^2J_{\text{P-P}} = 28$ Hz) and -0.63 ppm ($^1J_{\text{Pt-P}} = 2218$ Hz, $^2J_{\text{P-P}} = 28$ Hz). The patterns of the dppp signals in the ^1H and ^{13}C NMR spectra of the complex are affected by the lowered symmetry of their close environment similarly as in **9**. HR ESI-IMS results show four major peak envelopes corresponding to the tetracation **8** and to the dication of one-half of the molecule (m/z 847.7), a dinuclear fragment with two ligands **6** (dication, 937.7), an ion pair of NO_3^- with a tetranuclear fragment with one ligand **6** missing (trication, 1090.9), and a **8** - NO_3^- ion pair (trication, 1150.9). As with **9**, no higher charge signals were detected, nor any signals above $m/z = 1200$ (Figures S58-S62 in the Supplementary Information).

Encouraged by the success with rod **1**, and in analogy to the conversion of 1,3,5-tris(4-pyridylethynyl)benzene to a hexanuclear prismatic complex,²⁴ we attempted to prepare a three-dimensional block-shaped octanuclear complex by treating 5,10,15,20-tetra(4-pyridyl)-21*H*,23*H*-porphyrin with **1** in a 1:2 ratio. However, instead of the expected octanuclear complex, the remarkable tetranuclear planar complex **11** was isolated.

The ^1H NMR spectrum of this product did not have the expected symmetry. The signals of the pyrrole protons were split into two peaks of equal intensity and one of them was shifted far upfield, from 8.45 to 5.84 ppm. The resonances of the triptycene protons were split into four multiplets with relative intensities 2:2:1:1 instead of the expected two sets of multiplets of equal intensity. A comparison of solid state structure of the starting rod **1** with that of tetrapyrrolylporphyrin²⁷ revealed a similarity between its Pt-Pt separation (11.97 Å) and the lateral N-N distance between two pyridyl groups in the porphine (10.93 Å). This suggested that the unusual NMR shifts and splittings observed in **11** could be explained by a tetranuclear complex structure in which two units of **1** are coordinated laterally to the porphyrin. The shielding of the pyrrole protons by two benzene rings of a nearby triptycene would then cause the observed upfield shift of their ^1H NMR resonance. The proximity of the triptycene to the porphyrin would also block the free rotation of the former about its threefold axis and lead to the observed splitting of its signals in the ^1H NMR spectrum.

Ultimately, a single-crystal X-ray diffraction study of **11** on a synchrotron confirmed the correctness of these arguments (see Figure 2 for an ORTEP image of the structure). The very small single crystals available belonged to monoclinic $P2_1/n$ group. The structural unit contains two molecules of **11**, eight molecules of DMF and four molecules of water, all of them distorted. The coordination environment of platinum is slightly distorted in order to fit the demands of the porphine ligand. The C-Pt-N angle of $\sim 83^\circ$ contrasts with the $\sim 89^\circ$ C-Pt-I angle in the structure of **1**. The position of the Pt corner deviates significantly from the triptycene threefold axis and the C=C-Pt angle is only $\sim 165^\circ$. The pyridyl groups of the porphine ligand are slightly tilted from their position in the free molecule, with the C-C-N angle of $\sim 173^\circ$ (see the Supplementary Information).

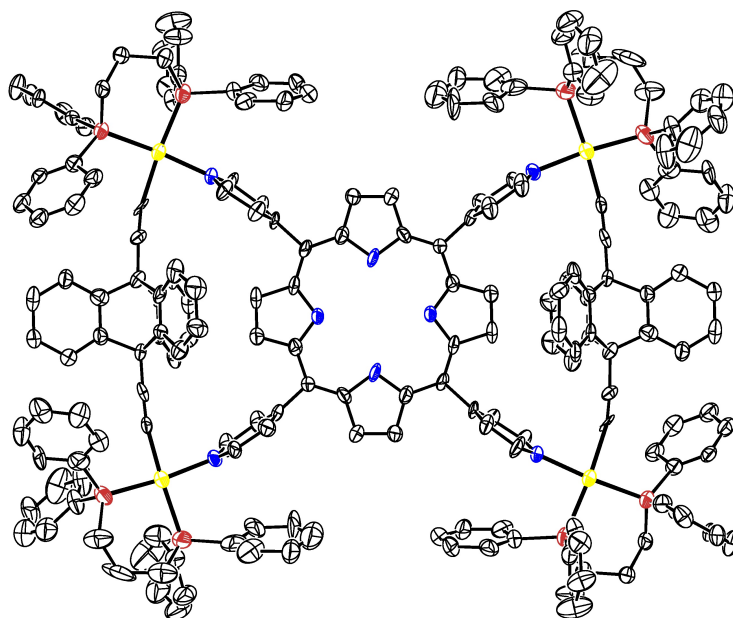


Figure 2. ORTEP drawing of **11** with 30% thermal probability ellipsoids (yellow: Pt, red: P, blue: N, black: C). Hydrogen atoms, solvent molecules (DMF), and atom labels were omitted for clarity.

Covalent Rectangles. Covalent stabilization of complexes **8** and **9** by treatment with 4,4'-diethynylbiphenyl (**12**) in 1:2 stoichiometric ratio under Sonogashira coupling conditions proceeded smoothly and the covalent rectangle **13** was obtained in excellent yields. However, the intermediacy of the non-covalent rectangles **8** or **9** is not necessary for efficient conversion of **1** to **13**. Starting with the double nitrate of **1** and one equivalent of **12**, very good yields of **13** were also obtained (Scheme 1).

It is equally possible to activate **1** for the synthesis of **13** by converting it to the double pyridine rod **14**, prepared similarly as **8** and **9** using pyridine instead of **6** or **7**. This rod has a diagnostic pattern in its ^{31}P NMR spectrum similar to those of **8** and **9**. A pair of P-P doublets ($^2J_{\text{P-P}} = 28$ Hz) with resonances at -12.79 ($^1J_{\text{Pt-P}} = 3132$ Hz) and -0.25 ppm ($^1J_{\text{Pt-P}} = 2207$ Hz) is assigned to P atoms trans to the pyridine and trans to the alkynyl, respectively. The ^1H and ^{13}C NMR spectra exhibit signal patterns due to the unsymmetrical dppp ligand similar to those of **8** and **9**.

There are two major peak envelopes in the ESI mass spectrum of **14**. They correspond to the molecular dication at $m/z = 836.7$ and to the ion pair of nitrate with a molecular fragment without one pyridine ligand at 1656.4. The isotopic pattern and the peak separations correspond to the calculated composition and charge of the fragments.

The poor solubility of **13** slightly hinders its characterization by NMR. Nevertheless, the results of the NMR analysis confirm the expected structure. An absolute assignment of the signals is not possible, because some are overlapped by solvent signals (especially some signals of phenyl rings and CH_2 groups of the dppp ligand). There are two resonances in the ^{31}P NMR spectrum of the complex (-5.77 and -5.75 ppm, $^1J_{\text{Pt-P}} \sim 2200$ Hz), but no P-P splitting is observed due to the close position and overlap of the signals in the spectrum. Also the ^1H and ^{13}C NMR

spectra reveal the overall symmetrization of the platinum coordination centers relative to the non-covalent macrocycles **8** and **9** or the rod **14** (Supplementary Information).

Crystals of **13** belong to the triclinic space group P1. The center of the rectangle is located at the inversion center, leaving almost 38% of the cell unit void. The cavity is filled with several very disordered molecules of the DMF solvent. The Pt corners of the rectangle are in a nearly ideal square planar arrangement and are slightly twisted, with the Pt-C≡C- bonds to triptycenes bent out of the rectangle and the Pt-C≡C- bonds to the biphenyls bent into the rectangle (Figure 3).

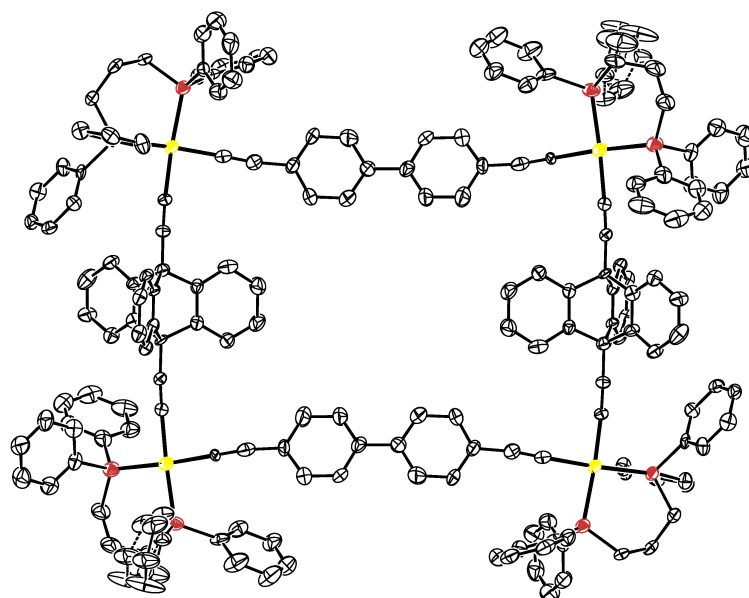
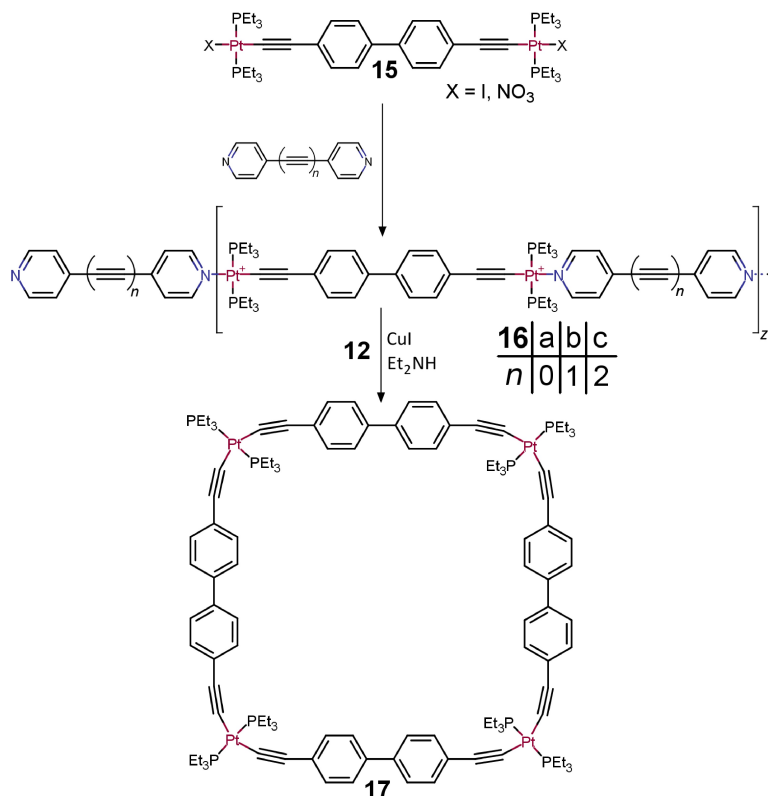


Figure 3. ORTEP drawing of **13** with 30% thermal probability ellipsoids (yellow: Pt, red: P, black: C). Hydrogen atoms, solvent molecules (DMF), and atom labels were omitted for clarity.

(ii) Trans Dialkynyl-Pt(II)-Bismonophosphine Macrocycles and Their Datively Bonded Precursors. An earlier brief communication¹⁶ on the ‘covalent stabilization’ process focused on the use of several pyridine-terminated rods as macrocycle-forming linkers (Scheme 3) and did not deal with the configuration at the Pt atoms. Only the Supporting Information reflected our automatic belief that the cis isomers are formed initially and isolated at the end, since the trans isomers would be too strained. It suggested that oddities in the number of ³¹P NMR signals and values of the ¹⁹⁵Pt-³¹P coupling constants could be due to ligand exchange processes.

We have now taken a closer look, reproduced the syntheses, prepared a set of model compounds, performed a series of density functional theory (DFT) calculations,²⁸ and realized that the automatic belief was incorrect. Isomers containing some cis Pt centers may be formed initially, but the isolated macrocycles have trans configuration at the Pt atoms and an unusual oval shape.



Scheme 3. Formation of complex **17**.

The reinterpretation of the NMR data for compounds **15** and **16a - 16c** in Scheme 3 as due to the trans isomers is straightforward and involves no irregularities. The single ^{31}P NMR signal of **15** with $^1J_{\text{Pt-P}} \sim 2300$ Hz is perfectly compatible with the trans structure,²⁶ and the data are also nicely compatible with originally unavailable results for a structure secured by single crystal X-ray diffraction.¹⁵

With this result in mind, the formation of the rectangular complexes **16** is improbable. A detailed examination of the products of the reaction of the nitrate complex **15** with the pyridine-terminated linkers by ^1H NMR (COSY, NOESY, DOSY) showed that macrocycles are not formed (Scheme 3). The results for **16a - 16c** were similar. Upon coordination to platinum, the signals of the α and β pyridyl protons in **6** move downfield from their initial values (e.g., 8.65 ppm and 7.43 ppm, respectively, in **16b**). Instead of the single signal for each expected in the macrocycle, the α and β pyridyl protons of **6** appear as six new signals in the product. In **16b**, the β proton at 7.92 ppm belongs to doubly coordinated **6**, that at 7.84 ppm belongs to the coordinated and the one at 7.46 ppm to the uncoordinated pyridyl of singly coordinated **6**. The intensity ratio of the latter two signals establishes the ratio of these two kinds of **6**, and thus the degree of oligomerization. For **16b**, the ratio was close to 3:1. Thus, on the average, the oligomer contains four Pt-Pt units joined through three ligands **6** and terminated with two additional molecules of **6**. DOSY was used to check that no free **6** was present. For **16a**, the ratio was 1:1 (two Pt-Pt units and three ligands **6** on the average), and for **16c**, it was 4:1 (five Pt-Pt units and six ligands **6** on the average).

These oligomers were subsequently used in the ‘covalent stabilization’ step and the previously reported products¹⁶ were obtained. Like that of **15**, the ^{31}P NMR spectrum of **17** is compatible with the presence of Pt atoms carrying two phosphines in trans positions ($^1J_{\text{Pt-P}} = 2360$ Hz) and ^1H NMR spectra contain only one set of signals of **12**. Terminal acetylene signals

are absent, showing that the product is cyclic. Previous size exclusion chromatography results¹⁶ and observations of solubility of model compounds, together with the HRMS results,¹⁶ suggest that the ring contains four Pt atoms.

Discussion

Four issues require comment. (i) The acceptor building blocks **1** and **5** both appear to be perfectly capable of producing covalent rectangular macrocycles in analogy to the prior synthesis of prismatic macrocycles built from a triptycene-containing rod.²⁴ Yet, while **1** produces macrocycles readily (Scheme 1), all attempts to form cycles with **5** yielded only linear oligomers or a polymer and no rectangles were isolated or detected (Scheme 2). In both cases, a syn attachment of new ligands on the Pt atoms appears necessary and sterically possible. We propose that the difference has to do with a difference in the ease with which the Pt termini rotate about the Pt-Pt axis to the syn conformation.

The large range of I-Pt-Pt-I dihedral angle values in X-ray diffraction crystal structures of **1** (Supporting Information) suggests that the triptycene bridge has no unfavorable steric interactions with the ligands on platinum. The nearly free rotation of the Pt(II)(dppp) moiety about the Pt-Pt axis then allows the desirable syn conformation to be reached easily and facilitates the macrocyclic ring closure.

The situation is different in **5**, where the trimethylsilyl groups carried by the rod would interfere with the diphenylphosphinyl moiety of the dppp ligand during an attempted rotation of the Pt(II)(dppp) moiety about the Pt-Pt axis. The anti geometry observed in the crystal structure is apparently favored but is not conducive to macrocycle formation, and the syn geometry is not being reached fast enough during the coupling process.

(ii) The unexpected isolation of the unusual tetranuclear planar complex **11** is presumably enabled by the compatible structural parameters of the porphine and the dinuclear rod and reveals how easily the alkyne moiety bends to accommodate structural requirements elsewhere. In **11**, the normally facile rotation of triptycene about its threefold axis appears to be suppressed entirely.

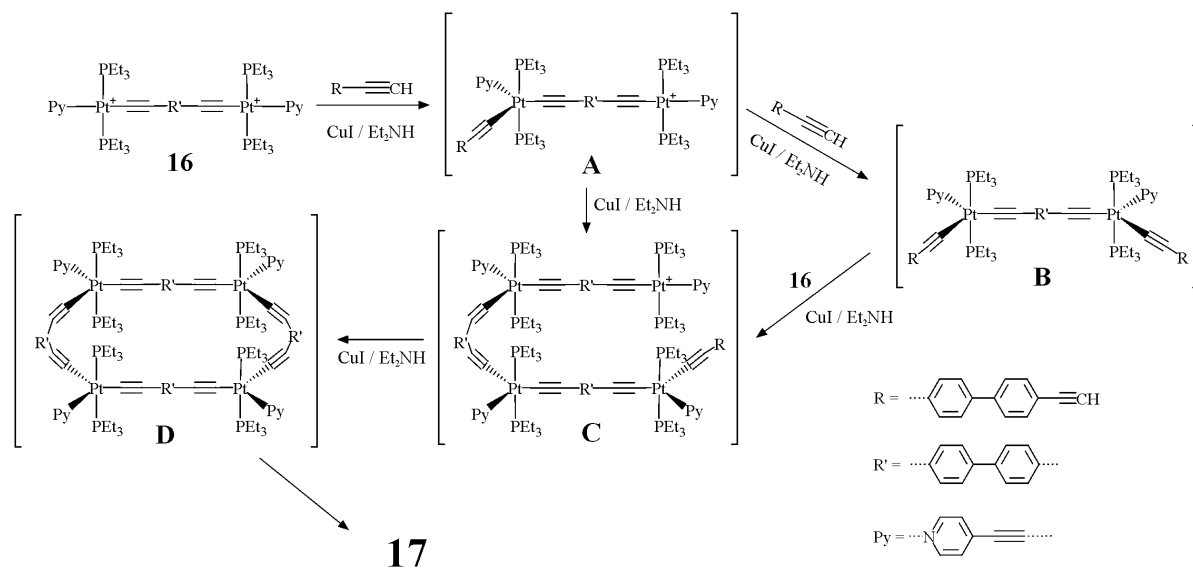
(iii) Given the essentially free rotation of the cis Pt centers about the rod axis in **1**, it is intuitively understandable that the self-assembly of **1** with **6** or **7** is able to produce charged rectangles **8** and **9**, while the combination of **1** or **14** with **12** produces the neutral rectangle **13** (Scheme 1). We have suggested above that a barrier to such rotation in **5** provides an explanation for the exclusive formation of linear oligomers from **5** and **6** or **7** (Scheme 2).

The self-assembly of **15** with **6** or **7** yields exclusively the linear oligomers **16** (Scheme 3), and this is perhaps not surprising considering that the trans form on Pt is more stable than cis and the concentration of **6** or **7** is fairly high. In contrast, the self-assembly of **12** with **14** or activated **1** furnishes the macrocycle **13** (Scheme 1), but in this case the necessary cis geometry at Pt is enforced by the diphosphine ligand and high dilution is used. The charged macrocycles are formed more reluctantly than the electroneutral ones. It is also possible that the electrostatic repulsion of positive charges, only partly compensated by counterions, destabilizes the cyclic form.

(iv) The covalent tetranuclear rectangle **13**, in which a cis geometry is secured by the use of a diphosphine, is accessible in the same good to excellent yields from reaction of **12** with **1**, as long as the latter is activated with AgNO₃. The reaction can be performed either directly or via **8**, **9**, or **14** (Scheme 1). We conclude that a preformation of a rectangle with a pyridine-terminated ligand¹⁶ is not necessary for the successful formation of the covalent rectangle. Without activation with AgNO₃, however, the yield is lower. It is possible that under the reaction conditions used, the self-assembly is reversible and the reaction actually is under thermodynamic control.

The configuration of the macrocyclic product is different when two monophosphines

are present on each Pt atom instead and the cis geometry is thus not enforced (Scheme 3). The initial activation by placement of pyridine residues on the Pt atoms produces a linear and not a macrocyclic product when doubly pyridine-terminated rods are used, and yet, after covalent stabilization, the macrocyclic covalent product **17** is formed in the end. However, judging by NMR spectra, instead of a rectangle with four cis ligated Pt atoms, an intriguing oval with four trans ligated Pt atoms is formed, and DFT calculations²⁸ agree that the all-trans configuration is much more stable than the originally expected all-cis. It is unfortunate that all our attempts to grow a suitable single crystal for diffraction analysis have failed.



Scheme 4. A mechanism suggested for formation of **17** via several intermediates containing trigonal bipyramidal Pt coordination centers. The bond angles in **C** and **D** are exaggerated, and in reality the Pt-C-C bond angle may deviate by up to 10° from linearity (cf. the structure of complexes **1**, **5**, **11**, and **13**).

The mechanism of the macrocyclization that yields **17** is presently not known and we hesitate to speculate about it excessively. It seems unlikely that the reactive ends of a linear oligomer with all-trans ligated Pt atoms would find each other to form a cycle, and it is more probable that the coupling process proceeds by an associative mechanism that enables cyclization in a temporary structure that contains trigonal bipyramidal Pt atoms and places the reactive ends of the oligomer much closer to each other. Scheme 4 depicts a possible cyclization pathway involving several trigonal-bipyramidal intermediates. A lifetime of the intermediate **A** has to be sufficiently long either to react with another molecule of complex **16** to form the intermediate **B**, with both metal centers remaining trigonal bipyramidal, or to react with another molecule of **A** to form the intermediate **C**. The presence of a Cu(I) salt in the reaction mixture could be beneficial in that an interaction of Cu(I) with the π -electrons of both alkynes could extend the lifetime of intermediates such as **B** or **C**.²⁹ We presume that the presence of two alkynes in these intermediates is crucial for the stabilization. Subsequent cyclization reaction between two ends of complex **C** then leads to **D**, and reversion of the Pt atoms to square planar geometry yields **17**, which precipitates from the solution. The all-trans configuration is not formed until after the macrocycle has been closed. Regardless of the mechanism of formation, the structure of the all-trans macrocycle is intriguing.

The competition between suffering mechanical strain by bending structural elements such as triple bonds that would prefer to remain linear and suffering electronic strain by placing phosphine ligands into a cis configuration is clearly won by the latter, and both the calculated

and the observed preference is for the all-trans and not the all-cis macrocycle. The situation is discussed further in a separate article based on DFT calculations.²⁸

Conclusions

This work has produced three significant results. The first is a finding that the structure of the charged complexes formed upon reaction of **1** or **5** with **6** or **7** is determined by the type of the connecting dialkyne ligand. Excessively bulky functional groups, such as the trimethylsilyl groups in **5**, hinder free rotation of the platinum termini decorated with the dppp ligands and prevent a rearrangement of the molecule to a shape favorable to formation of a rectangular product; open chain oligomers are formed instead. In contrast, the triptycene linker in **1** introduces no such constraints on the rearrangement of the complex and tetranuclear rectangular platinum macrocycles are formed under the same reaction conditions. These charged rectangular complexes can be converted to neutral compounds upon reaction with **12**. Surprisingly, the same products are obtained upon reaction of the rod **1** or the non-cyclic charged complex **14** with **12**.

Second, an attempted preparation of a 'three-dimensional' octanuclear platinum complex resulted in an unexpected formation of the flat polycyclic complex **11** due to a coincidental match of the dimensions of **1** and **10**. Although the match is only approximate, the flexibility of the system makes formation of the complex **11** possible and even preferable over formation of complexes with more porphine molecules linked together.

The third intriguing and most surprising result is the formation of the tetranuclear all-trans ring complex **17** from linear charged oligomers. Although the originally expected geometry of this compound was all-cis,¹⁶ the additional experimental and computational work convinced us that the arrangement of the ligands on the platinum coordination centres is all-trans.

Experimental Section

Preparation of the starting materials, 4,4'-diethynylbiphenyl (**12**),³⁰ 1,2-di(pyridin-4-yl)ethyne (**6**),³¹ 1,4-di(pyridin-4-yl)buta-1,3-diyne (**7**),³² [PtMe₂(1,5-COD)],³³ and 1,4-bis(trimethylsilyl)-2,5-diethynylbenzene³⁴ followed published procedures. *Cis*-(dppp)(I)Pt(C≡C-triptycene-C≡C)Pt(I)(dppp) (**1**) was prepared and converted to *cis*-(dppp)(NO₃)Pt(C≡C-triptycene-C≡C)Pt(NO₃)(dppp) as previously described.²⁴ The solvents, diethylamine, triethylamine, and the inorganic salts were purchased and distilled over CaH₂ (dichloromethane), P₄O₁₀/Na-K alloy (THF), sodium (toluene) or KOH (HNEt₂, HNi-Pr₂, Et₃N). K₂PtCl₄, dppm, dppe and dppp were purchased from Strem Chemicals Inc. Other reagents were purchased from Sigma-Aldrich and used as received. Deuterated solvents were purchased from Eurisotop, Saclay, France.

NMR spectra were recorded with Bruker AVANCE III spectrometers operating at 300, 400, 500, and 600 MHz at room temperature (25° C) unless stated otherwise. ¹H and ¹³C spectra were referenced to residual solvent peaks.

Crystals for structure determination by X-ray diffraction were prepared as follows. Single crystals of **1** were grown from a methylene chloride solution either by vapor diffusion of THF into it (**1a**) or by slow solvent evaporation (**1b**), those of **5** were grown upon slow cooling of a warm solution in DMF-*d*₇, those of **11** were grown from its saturated DMF solution by hexane vapor diffusion, and those of **13** grew from a DMF solution upon standing.

Crystallographic data for all the complexes except **11** were collected on Nonius KappaCCD diffractometer equipped with Bruker APEX-II CCD detector by monochromatized MoK α radiation ($\lambda = 0.71073 \text{ \AA}$) at a temperature of 150(2) K. The structures were solved by direct methods (SHELXT)³⁵ and refined by full matrix least squares based on F^2 (SHELXL98).³⁶ The hydrogen atoms were calculated into idealized positions and were refined as fixed (riding

model) with assigned temperature factors $H_{\text{iso}}(\text{H}) = 1.2 U_{\text{eq}}(\text{pivot atom})$ or $1.5 U_{\text{eq}}$ (methyl groups). It was necessary to remove the contribution of the disordered solvent molecules to the diffraction pattern during the refinement of structures **1a**, **1b**, and **13** using the PLATON/SQUEEZE³⁷ procedure. For the structures **1a** and **13**, also constraints on displacement parameters of all the carbon atoms were applied. However, the poor quality of the crystal of **1a** still affects the precision of the final structure and the structure thus does not pass the evaluation procedure without serious alerts and the respective .cif file can be found as a part of the Supporting Information.

Crystallographic data for **11** were collected on a Bruker D8 diffractometer equipped with a PHOTON100 CMOS detector and Oxford Cryosystems Cryostream 700 plus, on Beamline 11.3.1 of the Advanced Light Source at Lawrence Berkeley National Laboratory. A sphere of data were collected at 100 K using Bruker APEX³⁸ software in shutterless mode with ω rotations at fixed Φ values at $\lambda = 0.7749 \text{ \AA}$, from a channel cut Silicon [111] monochromator. The intensity data were integrated and correction applied with SAINT v8.38a,³⁹ absorption and other corrections were made using SADABS 2016/2.⁴⁰ Dispersion corrections appropriate for this wavelength were calculated using the Brennan method in XDISP⁴¹ with WinGX.⁴² The structures were solved with a dual space method with SHELXL 2014/4³⁵ and refined using SHELXL 2014/7.³⁵ Hydrogen atoms were placed geometrically where possible and added using HFIX 137 on the DMF solvent molecules constrained and refined using a riding model. The hydrogen atoms were placed on the nitrogen with the most symmetrical bonding in the porphyrin. The hydrogen atoms on the water molecules could not be found in the difference map and therefore omitted from the refinement but not the chemical formula.

ESI-IMS experiments were performed with a Synapt G2 Q-ToF mass spectrometer (Waters, UK) fitted with an electrospray ionization source. Dilute solutions (2 mg L^{-1}) in chloroform were introduced into the ESI source via a fused-silica capillary at a flow rate of 0.6 mL h^{-1} . Nitrogen was used as the nebulizer gas. The operating conditions for the ion-trap mass spectrometer were: capillary voltage 3.5 kV, sampling and extraction cone 38 and 4 V, source and desolvation temperature 100 and 350°C and cone and desolvation gas 50 and 450 L h^{-1} . Mass spectra were recorded from m/z 50 to 1200 (2000). The collision cross section Ω (collision momentum transfer integral) was determined using spectral calibration based on polyalanine IMS separation.

Combustion elemental analysis (CHNS-O) was performed using a PE 2400 Series II CHNS/O Analyzer (Perkin Elmer, USA) in the CHN operating mode (the most robust and interference-free mode) to convert the sample elements to simple gases (CO_2 , H_2O and N_2). The PE 2400 analyzer automatically performed combustion, reduction, homogenization of product gases, separation and detection. An MX5 microbalance (Mettler Toledo) was used to weigh the samples (1.5–2.5 mg per single sample analysis). Using this procedure, the accuracy of CHN determination is better than 0.30% abs. Internal calibration was performed using *N*-phenylurea. Platinum content was determined using X-ray fluorescence analyzer Spectro iQII (Spectro Analytical Instruments Inc., USA).

1,4-Bis({[1',3'-bis(diphenylphosphino)propane](iodo)platinum(II)}ethynyl)-3,5-bis(trimethylsilyl)benzene (5). *Cis*-(dppp)PtI₂ (3.9 g, 4.5 mmol, 4 eq) was suspended in 450 mL of freshly distilled methylene chloride in a dry round-bottom flask (1 L). 1,4-bis(trimethylsilyl)-2,5-diethynylbenzene (300 mg, 1.11 mmol, 1 eq) dissolved in 10 mL of freshly distilled methylene chloride was added, followed by freshly distilled diethylamine (126 mL), and the suspension was stirred at room temperature for 20 min. CuI (66 mg, 10 mol%) was added at once and the mixture was stirred for 48 h at room temperature. The reaction mixture was concentrated to half of its original volume and 300 mL of hexane were added under vigorous stirring to precipitate the product together with the remaining starting material and the diethylammonium iodide side product. The precipitate was filtered off, washed with hexane, and

air dried. The dry powder was suspended in 150 mL of distilled water and stirred for 30 min to ensure dissolution of the diethylammonium salt. The remaining solid material was filtered off, washed by acetone and air dried. The dry powder was suspended in 100 mL of methylene chloride and sonicated for 5 min. As the product is only sparingly soluble in this solvent, it remained undissolved and was filtered, washed with methylene chloride (3 × 10 mL) and then 20 mL of diethyl ether, and air dried. Yellowish powder (1 g, 52% yield). ¹H NMR (500 MHz, DMF-*d*₇, 120°C) δ = 7.97 (m, 8H), 7.84 (m, 8H), 7.46 (m, 18H), 7.39 (m, 8H), 2.74 (m, 8H), 2.06 (m, 4H), 0.22 (s, 18H) ppm. ¹³C {¹H} NMR (126 MHz, DMF-*d*₇, 120°C) δ = 139.8, 137.7, 135.4 (d, *J* = 9.9 Hz), 134.6 (d, *J* = 10.6 Hz), 133.7 (d, *J* = 55.4 Hz), 132.2 (d, *J* = 63.1 Hz), 131.8, 131.5, 130.7, 129.2 (d, *J* = 11.2 Hz), 129.0 (d, *J* = 10.5 Hz), 117.1 (d, *J* = 30.0 Hz), 107.8 (dd, *J* = 153.0, 13.9 Hz), 26.7 (dd, *J* = 36.7, 6.9 Hz), 26.3 (dd, *J* = 33.0, 5.0 Hz), 20.5, 0.7 ppm. ³¹P {¹H} NMR (202 MHz, DMF-*d*₇, 120°C) δ = -13.01 (d, *J*_{P-P} = 25 Hz, *J*_{Pt-P} = 2174 Hz), -14.45 (d, *J*_{P-P} = 25 Hz, *J*_{Pt-P} = 3364 Hz). Anal. (%) Calcd. for C₇₀H₇₂I₂P₄Pt₂Si₂: C, 48.39; H, 4.18; Pt, 22.46. Found: C, 48.15; H, 4.14; Pt, 21.35

Triptycene-dipyridylacetylene Rectangle (8). Complex **1** (50 mg, 28 μmol) and **6** (5.1 mg, 28 μmol) were dissolved in dry methylene chloride (150 mL) in an aluminum foil-wrapped flask. To the stirred solution silver(I) nitrate (9.6 mg, 57 μmol) was added and the slurry was stirred in the dark at room temperature overnight. Precipitated silver(I) iodide was removed by filtration through a Whatman 0.2 μm filter and the filtrate was concentrated under reduced pressure to provide a quantitative yield (50 mg) of a light yellow solid. Mp = 245 – 250 °C (dec). ¹H NMR (400 MHz, DMF-*d*₇): δ = 8.99 – 8.82 (m, 8H), 8.23 (dd, 12.3 Hz, 6.7 Hz, 16H), 7.73 (dd, 11.4 Hz, 7.5 Hz, 16H), 7.73 (dd, 11.4 Hz, 7.5 Hz, 16H), 7.66 – 7.54 (m, 32H), 7.51 (d, 6.1 Hz, 8H), 7.48 – 7.33 (m, 16H), 6.78 – 6.72 (m, 12H), 6.66 – 6.60 (m, 12H), 3.32 – 3.17 (m, 8H), 3.13 – 2.98 (m, 8H), 2.22 – 1.99 (m, 8H). ¹³C {¹H} NMR (100 MHz, DMF-*d*₇): δ = 152.0, 145.0, 134.1, 134.0, 133.9, 133.8, 132.2, 131.8, 130.0, 129.4, 129.3, 129.2, 128.8, 128.5, 128.2, 124.8, 122.1, 97.6, 97.3, 91.8, 24.9 (d, ²*J*_{C-P} = 36 Hz), 23.0 (d, ²*J*_{C-P} = 36 Hz), 19.1. ³¹P {¹H} NMR (162 MHz, DMF-*d*₇): δ = -0.63 (d, ³*J*_{P-P} = 28 Hz, ¹*J*_{P-Pt} = 2218 Hz), -10.65 (d, ³*J*_{P-P} = 28 Hz, ¹*J*_{P-Pt} = 3152 Hz). ¹⁹⁵Pt NMR (64.5 MHz, DMF-*d*₇): δ = -4595 (dd, ¹*J*_{P-Pt} = 2218, 3152 Hz). HRMS: calcd. for C₁₈₀H₁₄₄N₄P₈Pt₄ 847.1965, found (ESI+) 847.1912 ([M⁴⁺]). Anal. (%) Calcd. for C₁₈₀H₁₄₄N₈O₁₂P₈Pt₄: C, 59.41; H, 3.99; N, 3.08; Pt, 21.44. Found: C, 59.17; H, 3.95; N, 3.01; Pt, 20.95.

Triptycene-dipyridylbutadiyne Rectangle (9). Dry methylene chloride (160 mL) was cannulated to a dry mixture of **1** (106 mg, 0.06 mmol) and silver(I) nitrate (21 mg, 0.12 mmol). After stirring overnight under inert conditions in a flask wrapped with aluminum foil, **7** (12 mg, 0.06 mmol) was added. After 15 h, the mixture was filtered through a Whatman 0.2 μm filter and concentrated under reduced pressure. Beige solid (110 mg, 99%). Mp = 235 – 240 °C (dec). ¹H NMR (400 MHz, DMF-*d*₇): δ = 8.98 – 8.86 (m, 8H), 8.30 – 8.15 (m, 16H), 7.81 – 7.71 (m, 16H), 7.66 (d, 8H, *J* = 6.2 Hz), 7.65 – 7.55 (m, 24H), 7.55 – 7.49 (m, 8H), 7.45 – 7.38 (m, 16H), 6.74 – 6.69 (m, 12H, *J* = 5.4, 3.3 Hz), 6.67 – 6.61 (m, 12H, *J* = 5.4, 3.4 Hz), 3.29 – 3.18 (m, 8H), 3.10 – 2.99 (m, 8H), 2.20 – 2.01 (m, 8H). ¹³C {¹H} NMR (126 MHz, DMF-*d*₇): δ = 152.9, 145.9, 134.8 (d, ²*J*_{C-P} = 10.7 Hz), 134.6 (d, ²*J*_{C-P} = 10.7 Hz), 133.0, 132.6, 131.7, 130.7, 130.2 (d, ³*J*_{C-P} = 11.0 Hz), 130.0 (d, ³*J*_{C-P} = 11.2 Hz), 129.5, 129.1, 111.1 (dd, H, *cis*-²*J*_{C-P} = 135.2, *trans*-²*J*_{C-P} = 14.1 Hz), 98.1 (d, ³*J*_{C-P} = 30.0 Hz), 81.2, 79.6, 54.1, 25.8 (d, ¹*J*_{C-P} = 40.7 Hz), 23.8 (d, ¹*J*_{C-P} = 34.7 Hz), 19.9. ³¹P {¹H} NMR (202 MHz, DMF-*d*₇): δ = -10.63 (d, ²*J*_{P-P} = 28 Hz, ¹*J*_{P-Pt} = 3142 Hz), -0.54 (d, ²*J*_{P-P} = 28 Hz, ¹*J*_{P-Pt} = 2210 Hz). ¹⁹⁵Pt NMR (107 MHz, DMF-*d*₇): δ = -4593 (dd, ¹*J*_{P-Pt} = 2215, 3162 Hz). HRMS: calcd. for C₁₈₄H₁₄₄N₄P₈Pt₄ 859.1965, found (ESI+) 859.3018. Anal. (%) Calcd. for C₁₈₄H₁₄₄N₈O₁₂P₈Pt₄: C, 59.94; H, 3.94; N, 3.04; Pt, 21.16. Found: C, 59.76; H, 3.90; N, 2.99; Pt, 20.87.

Triptycene-tetrapyridylporphine Rectangle (11). Complex **1** (40 mg, 22.6 μmol) was dissolved in dry methylene chloride (100 mL) in an aluminum foil-wrapped flask. 5,10,15,20-

tetra(4-pyridyl)-21*H*,23*H*-porphyrin (7 mg, 11.3 μmol) and silver(I) nitrate (8 mg, 43 μmol) were added and the mixture was stirred under argon atmosphere in the dark for 48 h. The silver(I) iodide precipitate was filtered off using a Whatman 0.2 μm filter and the filtrate was concentrated under reduced pressure. Violet powder (40 mg, 97% yield). Mp = 243 – 247 $^{\circ}\text{C}$ (dec). ^1H NMR (500 MHz, DMF- d_7): δ = 8.96 (dt, 8H, J = 4.4, 2.7 Hz), 8.45 (s, 4H), 7.99 – 7.88 (m, 16H), 7.79 (d, 8H, J = 5.5 Hz), 7.73 – 7.62 (m, 16H), 7.45 (dt, 8H, J = 7.0, 3.5 Hz), 7.43 – 7.38 (m, 8H), 7.35 – 7.27 (m, 40H), 6.21 (dd, 8H, J = 5.5, 3.2 Hz), 6.17 (dd, 4H, J = 5.4, 3.2 Hz), 5.84 (s, 4H), 5.71 (dd, 4H, J = 5.4, 3.2 Hz), 3.06 – 3.15 (m, 8H), 2.77 – 2.88 (m, 8H), 2.06 – 1.87 (m, 8H). $^{13}\text{C}\{^1\text{H}\}$ NMR (126 MHz, DMF- d_7): δ = 153.2, 150.8, 146.4, 145.3, 134.9 (d, $^2J_{\text{C-P}} = 10.6$ Hz), 134.6 (d, $^2J_{\text{C-P}} = 10.6$ Hz), 133.0, 132.8, 131.5, 130.8, 130.2 (d, $^3J_{\text{C-P}} = 10.4$ Hz), 130.1, 130.0 (d, $^3J_{\text{C-P}} = 11.4$ Hz), 129.7, 125.8, 125.7, 123.6, 123.0, 112.9 (dd, *cis*- $^2J_{\text{C-P}} = 136.8$, *trans*- $^2J_{\text{C-P}} = 13.8$ Hz), 99.2 (d, $^3J_{\text{C-P}} = 30.4$ Hz), 54.6, 25.7 (d, $J_{\text{C-P}} = 39.3$ Hz), 23.4 (d, $J_{\text{C-P}} = 36.0$ Hz), 20.2. $^{31}\text{P}\{^1\text{H}\}$ NMR (162 MHz, DMF- d_7): δ = 2.7 (d, $J_{\text{P-P}} = 27.4$ Hz, $^1J_{\text{Pt-P}} = 2204$ Hz), -7.9 (d, $J_{\text{P-P}} = 27.4$ Hz, $^1J_{\text{Pt-P}} = 3156$ Hz). HRMS: calcd. for $\text{C}_{196}\text{H}_{154}\text{N}_8\text{P}_8\text{Pt}_4$ 911.7192, found (ESI+) 911.8331. Anal. (%) Calcd. for $\text{C}_{196}\text{H}_{154}\text{N}_8\text{P}_8\text{Pt}_4$: C, 64.51; H, 4.25; N, 3.07; Pt, 21.38. Found: C, 64.27; H, 4.31; N, 3.23; Pt, 21.17.

Triptycene-diethynylbiphenyl Rectangle (13). Dry methylene chloride (30 mL) was cannulated to a dry mixture of **1**, **9** (0.01 mmol) or **14** (0.005 mmol), **12** (0.01 mmol) and cuprous iodide (10 mg). After cooling to -25°C , triethylamine (1 mL) was added and the mixture was warmed to room temperature and stirred overnight. The solution was extracted twice with water (10 mL) and washed twice with brine (10 mL). The organic phase was dried over sodium sulfate and evaporated under reduced pressure. Beige-white solid, yields from **1**, **9**, and **14**: 64%, 100%, and 96%, respectively. Mp > 350 $^{\circ}\text{C}$. ^1H NMR (400 MHz, DMF- d_7): δ = 8.12 (m, 32H), 7.52 (m, 60H), 2.03 (m, 8H), 7.38 (d, 8H, $^3J_{\text{H-H}} = 8$ Hz), 6.89 (d, 8H, $^3J_{\text{H-H}} = 8$ Hz), 6.75 (m, 12H), 2.89 (m, 8H, overlap with DMF- d_7), 2.83 (m, 8H, overlap with DMF- d_7), 2.05 (m, 8H). ^{13}C NMR (101 MHz): δ = 146.4, 137.0, 134.4 (d, $^2J_{\text{C-P}} = 9$ Hz), 134.1 (d, $^2J_{\text{C-P}} = 9$ Hz), 132.8, 132.2, 131.6, 131.0, 130.8, 129.8, 128.7 (d, $^3J_{\text{C-P}} = 10$ Hz), 128.6 (d, $^3J_{\text{C-P}} = 10$ Hz), 125.7, 124.5, 123.0, 108.6 (HMBC), 53.9 (HMBC), 26.0 (HSQC), 25.3 (HSQC), 20.3. ^{31}P NMR (162 MHz): δ = -5.75 (s, $^1J_{\text{P-Pt}} = 2212$ Hz), -5.77 (s, $^1J_{\text{P-Pt}} = 2212$ Hz). ^{195}Pt NMR (64.5 MHz): δ = -4884 (dd, $^1J_{\text{P-Pt}} = 2257$ Hz). Anal. (%) Calcd. For $\text{C}_{194}\text{H}_{158}\text{N}_2\text{O}_2\text{P}_8\text{Pt}_4$: C, 65.13; H, 4.45; N, 0.78; Pt, 21.81. Found: C, 64.97; H, 4.39; N, 0.82; Pt, 21.69.

Triptycene-9,10-diethynylbis(cis-[[bis(diphenylphosphino)propane](pyridine)platinum(II)]nitrate) (14). Dry methylene chloride (80 mL) was cannulated to a dry mixture of **1** (106 mg, 0.06 mmol) and silver(I) nitrate (21 mg, 0.12 mmol). After stirring overnight under inert conditions in a flask wrapped in an aluminum foil, 35 μL of anhydrous pyridine were added. After 15 h, the mixture was filtered through a Whatman 0.2 μm filter and concentrated under reduced pressure. White solid (107 mg, 97%). Mp > 258 – 264 $^{\circ}\text{C}$ (dec). ^1H NMR (300 MHz, CD_2Cl_2): δ = 8.51 – 8.33 (m, 4H), 8.08 – 7.95 (m, 8H), 7.59 (m, 2H), 7.54 – 7.42 (m, 20H), 7.42 – 7.34 (m, 4H), 7.31 – 7.20 (m, 8H), 7.13 – 7.04 (m, 4H), 6.68 – 6.60 (m, 6H), 6.60 – 6.52 (m, 6H), 3.04 – 2.91 (m, 4H), 2.85 – 2.73 (m, 4H), 2.25 – 1.98 (m, 4H). $^{13}\text{C}\{^1\text{H}\}$ NMR (75 MHz, CD_2Cl_2): δ = 151.7, 145.12, 139.1, 133.9 (d, $^2J_{\text{C-P}} = 18$ Hz), 133.7 (d, $^2J_{\text{C-P}} = 18$ Hz), 132.4 (d, $^4J_{\text{C-P}} = 4$ Hz), 130.0, 129.7 (d, $^3J_{\text{C-P}} = 12$ Hz), 129.51 (d, $^3J_{\text{C-P}} = 13$ Hz), 129.1, 128.7, 128.0, 126.8, 125.1, 122.3, 53.1, 25.5 (d, $^2J_{\text{C-P}} = 36$ Hz), 24.2 (d, $^2J_{\text{C-P}} = 36$ Hz), 19.6. $^{31}\text{P}\{^1\text{H}\}$ NMR (122 MHz, CD_2Cl_2): δ = -0.43 (d, $^3J_{\text{P-P}} = 28$ Hz, $^1J_{\text{P-Pt}} = 2207$ Hz), -12.05 (d, $^3J_{\text{P-P}} = 28$ Hz, $^1J_{\text{P-Pt}} = 3132$ Hz). ^{195}Pt NMR (64.5 MHz, CD_2Cl_2): δ = -4578 (dd, $^1J_{\text{P-Pt}} = 2213$, 3150 Hz). MS (ESI+): m/z 1656.4 [(M – py + NO_3) $^+$, 13], 836.7 (M^{2+} , 100). Anal. (%) Calcd. for $\text{C}_{88}\text{H}_{74}\text{N}_4\text{O}_6\text{P}_4\text{Pt}_2$: C, 58.80; H, 4.15; N, 3.12; Pt, 21.70. Found: C, 58.53; H, 4.07; N, 3.09; Pt, 20.93.

Supporting Information. NMR spectra of compounds **5**, **8**, **9**, **11**, **13**, **14**, ESI-IMS

spectra of compounds **8**, **9**, **11**, crystallographic data of compounds **1**, **5**, **11**, **13**, and the .cif file of the compound **1a**.

Accession codes. CCDC 1953720, 1953719, 1950566, and 1953984 structures contain the crystallographic data of the structures **1b**, **5**, **11**, and **13**, respectively. These data can be obtained free of charge via http://www.ccdc.cam.ac.uk/data_request/cif, or by emailing data_request@ccdc.cam.ac.uk, or by contacting The Cambridge Crystallographic Data Centre, 12 Union Road, Cambridge CB2 1EZ UK; fax: +44 1223 336033.

Corresponding authors

*E-mail for J.M.: michlj@colorado.edu

ORCID

Jan Plutnar: 0000-0002-5580-3084

Cyprien Lemouchi: 0000-0002-2236-496X

Jana Dyrťová Jaklová: 0000-0002-6024-8679

Ivana Čiřářová: 0000-0002-9612-9831

Simon J. Teat: 0000-0001-9515-2602

Josef Michl: 0000-0002-4707-8230

Notes

The authors declare no competing financial interest.

Acknowledgement. Work in Boulder was supported by the U.S. National Science Foundation, DMR 1608424. Work in Prague was supported by the European Research Council under the European Community's Framework Programme (FP7/2007-2013) ERC grant agreement no 227756, and by the Institute of Organic Chemistry and Biochemistry, Academy of Sciences of the Czech Republic (RVO: 61388963). This research used resources of the Advanced Light Source, which is a DOE Office of Science User Facility under contract no. DE-AC02-05CH11231.

References

1. K. Sonogashira, T. Yatake, Y. Tohda, S. Takahashi, N. Hagihara, "Novel preparation of σ -alkynyl complexes of transition metals by copper(I) iodide-catalysed dehydrohalogenation", *J. Chem. Soc. Chem. Commun.* **1977**, 291-292.
2. K. Sonogashira, Y. Fujikura, T. Yatake, N. Toyoshima, S. Takahashi, N. Hagihara, "Syntheses and properties of *cis*- and *trans*-dialkynyl complexes of platinum(II)", *J. Organomet. Chem.* **1978**, *145*, 101-108.
3. C. J. Kuehl, C. L. Mayne, A. M. Arif, P. J. Stang, "Coordination-driven assembly of molecular rectangles via an organometallic 'clip'", *Org. Lett.* **2000**, *2*, 3727-3729.
4. W. Kaim, B. Schwederski, A. Dogan, J. Fiedler, C. J. Kuehl, P. J. Stang, "Metalla-supramolecular rectangles as electron reservoirs for multielectron reduction and oxidation", *Inorg. Chem.* **2002**, *41*, 4025-4028.

5. Y.-R. Zheng, H.-B. Yang, B. H. Northrop, K. Ghosh, P. J. Stang, "Size selective self-sorting in coordination-driven self-assembly of finite ensembles", *Inorg. Chem.* **2008**, *47*, 4706-4711.
6. Y.-R. Zheng, P. J. Stang, "Direct and quantitative characterization of dynamic ligand exchange between coordination-driven self-assembled supramolecular polygons", *J. Am. Chem. Soc.* **2009**, *131*, 3487-3489.
7. T. Megyes, H. Jude, T. Grósz, I. Bakó, T. Radnai, G. Tárkányi, G. Pálinkás, P. J. Stang, "X-ray diffraction and DOSY NMR characterization of self-assembled supramolecular metallocyclic species in solution", *J. Am. Chem. Soc.* **2005**, *127*, 10731-10738.
8. C. Addicott, I. Oesterling, T. Yamamoto, K. Müllen, P. J. Stang, "Synthesis of a bis (pyridyl)-substituted perylene diimide ligand and incorporation into a supramolecular rhomboid and rectangle via coordination driven self-assembly", *J. Org. Chem.* **2005**, *70*, 797-801.
9. M. J. E. Resendiz, J. C. Noveron, H. Disteldorf, S. Fischer, P. J. Stang, "A self-assembled supramolecular optical sensor for Ni (II), Cd (II), and Cr (III)", *Org. Lett.* **2004**, *6*, 651-653.
10. N. Das, P. S. Mukherjee, A. M. Arif, P. J. Stang, "Facile self-assembly of predesigned neutral 2D Pt-macrocycles via a new class of rigid oxygen donor linkers", *J. Am. Chem. Soc.* **2003**, *125*, 13950-13951.
11. N. Das, A. M. Arif, P. J. Stang, M. Sieger, B. Sarkar, W. Kaim, J. Fiedler, "Self-assembly of heterobimetallic neutral macrocycles incorporating ferrocene Spacer groups: Spectroelectrochemical analysis of the double two-electron oxidation of a molecular rectangle", *Inorg. Chem.* **2005**, *44*, 5798-5804.
12. N. Das, P. J. Stang, A. M. Arif, C. F. Campana, "Synthesis and structural characterization of carborane-containing neutral, self-assembled Pt-metallacycles", *J. Org. Chem.* **2005**, *70*, 10440-10446.
13. N. Das, A. Ghosh, O. M. Singh, P. J. Stang, "Facile synthesis of enantiopure chiral molecular rectangles exhibiting induced circular dichroism", *Org. Lett.* **2006**, *8*, 1701-1704.
14. N. Das, A. Ghosh, A. M. Arif, P. J. Stang, "Self-assembly of neutral platinum-based supramolecular ensembles incorporating oxocarbon dianions and oxalate", *Inorg. Chem.* **2005**, *44*, 7130-7137.
15. S. Shanmugaraju, S. A. Joshi, P. S. Mukherjee, "Self-assembly of metallamacrocycles using a dinuclear organometallic acceptor: synthesis, characterization, and sensing study", *Inorg. Chem.* **2011**, *50*, 11736-11745.
16. A. G. L. Olive, K. Parkan, C. Givélet, J. Michl, "Covalent Stabilization: A Sturdy Molecular Square from Reversible Metal-Ion Directed Self-Assembly", *J. Am. Chem. Soc.* **2011**, *133*, 20108-20111.
17. S. J. Lee, C. R. Luman, F. N. Castellano, W. Lin, "Directed assembly of chiral organometallic squares that exhibit dual luminescence", *Chem. Commun.* **2003**, *0*, 2124-

18. M. Janka, G. K. Anderson, N. P. Rath, "Synthesis of neutral molecular squares composed of bis(phosphine) platinum corner units and dialkynyl linkers. Solid-state characterization of $[\text{Pt}(\mu\text{-C}\equiv\text{C}\text{:C}\equiv\text{C})(\text{dppp})]_4$ ", *Organometallics* **2004**, *23*, 4382-4390.
19. N. J. Long, C. K. Wong, A. J. P. White, "Synthesis and spectroscopic and electronic characterization of new cis-configured di-to multiplatinum alkynyls", *Organometallics* **2006**, *25*, 2525-2532.
20. K. Campbell, R. McDonald, M. J. Ferguson, R. R. Tykwinski, "Using ligand exchange reactions to control the coordination environment of Pt (II) acetylide complexes: applications to conjugated metallacyclines", *J. Organomet. Chem.* **2003**, *683*, 379-387.
21. K. Campbell, C. A. Johnson, R. McDonald, M. J. Ferguson, M. M. Haley, R. R. Tykwinski, "A Simple, One Step Procedure for the Formation of Chiral Metallamacrocycles", *Angew. Chem. Int. Ed.* **2004**, *43*, 5967-5971.
22. A. J. Canty, T. Rodemann, B. W. Skelton, A. H. White, "Access to Alkynylpalladium(IV) and -Platinum(IV) species, including Triorgano(diphosphine)metal(IV) complexes and the structural study of an Alkynyl(pincer)platinum(IV) Complex, $\text{Pt}(\text{O}_2\text{CAr}_F)\text{I}(\text{C}\equiv\text{CSiMe}_3)(\text{NCN})$ ($\text{Ar}_F=4\text{-CF}_3\text{C}_6\text{H}_4$, $\text{NCN}=[2,6\text{-}(\text{dimethylaminomethyl})\text{phenyl-}N,C,M]$)", *Organometallics* **2006**, *25*, 3996-4001.
23. M. Wang, V. Vajpayee, S. Shanmugaraju, Y.-R. Zheng, Z. Zhao, H. Kim, P. S. Mukherjee, K.-W. Chi, P. J. Stang, "Coordination-driven self-assembly of M_3L_2 trigonal cages from preorganized metalloligands incorporating octahedral metal centers and fluorescent detection of nitroaromatics", *Inorg. Chem.* **2011**, *50*, 1506-1512.
24. D. C. Caskey, B. Wang, X. Zheng, J. Michl, "Self-assembled trigonal prismatic altitudinal rotors with triptycene paddle wheels", *Collect. Czechoslov. Chem. Commun.* **2005**, *70*, 1970-1985.
25. T. F. Magnera, J. Michl, "Altitudinal Surface-Mounted Molecular Rotors", *Topics in Current Chemistry*, Kelly, T. R., Ed. **2005** Springer-Verlag: Berlin, Germany, pp. 63-97.
26. P. S. Pregosin, R. W. Kunz, *³¹P and ¹³C NMR of Transition Metal Phosphine Complexes*, Springer-Verlag, Berlin Heidelberg, **1979**.
27. S. M. Yoon, I.-C. Hwang, K. S. Kim, H. C. Choi, "Synthesis of single-crystal tetra(4-pyridyl)porphyrin rectangular nanotubes in the vapor phase", *Angew. Chem. Int. Ed.* **2009**, *48*, 2506-2509.
28. E. A. Buchanan, J. Michl, unpublished results.
29. H. Lang, A. Jakob, B. Milde, "Copper(I) alkyne and alkynide complexes", *Organometallics*, **2012**, *31*, 7661-7693.
30. L. Liu, Z. Liu, W. Xu, H. Xu, D. Zhang, D. Zhu, "Syntheses, optical and electrochemical properties of 4, 4'-bis-[2-(3, 4-dibutyl-2-thienylethynyl)] biphenyl and its oligomers", *Tetrahedron* **2005**, *61*, 3813-3817.

31. H. L. Anderson, C. J. Walter, A. Vidal-Ferran, R. A. Hay, P. A. Lowden, J. K. M. Sanders, "Octatetrayne-linked porphyrins: 'stretched' cyclic dimers and trimers with very spacious cavities", *J. Chem. Soc. [Perkin 1]* **1995**, 2275-2279.
32. E. Merkul, D. Urselmann, T. J. J. Müller, "Consecutive one pot Sonogashira-Glaser coupling sequence – Direct preparation of symmetrical diynes by sequential Pd/Cu catalysis", *Eur. J. Org. Chem.* **2011**, 2011, 238-242.
33. R. Bassan, K. H. Bryars, L. Judd, A. W. G. Platt, P. G. Pringle, "Improved syntheses of [PtMe₂(1, 5-COD)]." *Inorganica Chim. Acta* **1986**, 121, L41-L42.
34. D. Lehnherr, J. Gao, F. A. Hegmann, R. R. Tykwinski, "Synthesis and electronic properties of conjugated pentacene dimers", *Org. Lett.* **2008**, 10, 4779-4782.
35. G. M. Sheldrick, "SHELXT – Integrated space-group and crystal-structure determination", *Acta Crystallogr. A*, **2015**, 71, 3-8.
36. G. M. Sheldrick, "Crystal structure refinement with SHELXL", *Acta Crystallogr. C*, **2015**, 71, 3-8.
37. A. L. Speck, "Structure validation in chemical crystallography", *Acta Crystallogr. D*, **2009**, 65, 148-155.
38. Bruker Apex2, *Bruker Analytical X-ray Systems Inc.*, Madison, WI, **2003**.
39. Bruker SAINT: SAX Area-Detector Integration Programm v 7.60a, *Bruker Analytical X-ray Systems Inc.*, Madison, WI, **2010**.
40. R. H. Blessing, "An Empirical Correction for Absorption Anisotropy,," *Acta Cryst. A*, **1995**, 51 (1), 33–38.
41. L. Kissel, R. H. Pratt, "Corrections to Tabulated Anomalous-Scattering Factors", *Acta Cryst. A*, **1990**, 46 (3).
42. L. J. Farrugia, "WinGX Suite for Small-Molecule Single-Crystal Crystallography", *J. Appl. Cryst.*, **1999**, 32 (4), 837–838.

